Design of a Specimen Geometry for the Tensile Testing of Small Samples

by

Ruochen Dong

B. S. in Engineering,
Anhui University of Technology, 2017

Submitted to the Graduate Faculty of

Swanson School of Engineering in partial fulfillment

of the requirements for the degree of

Master of Science in Mechanical Engineering

University of Pittsburgh

2019

UNIVERSITY OF PITTSBURGH

SWANSON SCHOOL OF ENGINEERING

This thesis was presented

by

Ruochen Dong

It was defended on

April 3, 2019

and approved by

Patrick Smolinski, PhD, Associate Professor,
Department of Mechanical Engineering and Materials Science

William Slaughter, PhD, Associate Professor
Department of Mechanical Engineering and Materials Science

Qing-Ming Wang PhD, Professor
Department of Mechanical Engineering and Materials Science

Thesis Advisor: Patrick Smolinski, PhD, Associate Professor

Design of a Specimen Geometry for the Tensile Testing of Small Samples

Ruochen Dong, M.S

University of Pittsburgh, 2019

The mechanical properties of biological tissues is important for different areas of research. However, due to the size of the tissue, only small tissue samples can be obtained. For this reason, this study focused on the development of a small tissue sample geometry for tensile testing. A sample geometry was designed based on ISO standard 527 and a cutting die was made by additive manufacturing machine. The performance of the die was assessed by testing with poultry tissue. Finally, a finite element model has been analyzed to study the stress distribution of the gage area of the specimen.

Table of Contents

List of Tables

List of Figures

Preface

First of all, I would like to extend my sincere to Dr. Patrick Smolinski for his willingness to be my research advisor. I have always looked up to him and have learnt a lot from him and his work within the short duration of my Master's degree program and finite element analysis class. I would also like to thank the University of Pittsburgh for providing me with excellent coursework and research facilities for my research work. Additionally, I would like to thank my friends Jingyi Liu who helped me with my thesis tables and figures and Chris Spicer who helped with making the punch and clamp.

Finally, my special thanks to Dr. William Slaughter and Dr. Qingming Wang for taking out the time to be on my Masters committee at such a short notice and providing me with valuable feedback.

All in all, it's a unique experience for me not only study abroad, but also follow many excellent professors. It will motivate me to pursue my dream.

1.0 Introduction

The mechanism of the living body had been a focus of study in human history and many scientists have made significant contributions to it. Schack August Steenberg Krogh won The Nobel Prize in Physiology or Medicine for his discovery of the capillary motor regulating mechanism in 1920 and Archibald Vivian Hill also won the Nobel prize for his discovery relating to the production of heat in the muscle. As Fung's definition, biomechanics is mechanics of biology[1]. Biomechanics is a branch of biophysics that applies quantitative principles and methods to the study of mechanical problems in living organisms. The research of biomechanics ranges widely and one of the most important fields is biosolid mechanics which study the mechanical behaviors of soft tissue materials in living organisms.

2.0 Background

"Tensile testing is a fundamental mechanical test used to determine the Young's modulus of elasticity and other tensile properties"[2]. Nowadays, there is an increasingly time patients are waiting for various suitable donate organ transplantations to treat failing or injured organs. Thus, an alternative is regenerative medicine which is trying to create material to restore damaged tissues. Therefore, it's necessary for the substitute materials to mimic the mechanics properties of the real soft tissue [3-4]. Mechanical properties can be obtained from testing which can include tensile test, compression test, three-point bending test and so on. However, there are many difficulties in tissue testing since the material is wet, slippery and soft, thus difficult to grip when applying loads. Additionally, the shape of test specimens is important since it is desired to get the true mechanical properties. On the other hand, the size of each specimen depends on the source of the test material. Thus, there are benefits to making the sample size as small as possible.

2.1 Study of mechanical properties of soft tissue

Many pieces of research focus on different soft tissues with different external factors and different internal factors and thus will have different results. Tensile testing may focus on stiffness, ultimate tensile strength, failure strength or maximum elongation. External factors can be time, temperature, strain rate, or other factors. Additionally, soft tissues can exhibit significant viscoelastic behavior, which is a significant property of biomaterials. One viscoelastic property is the loss factor $\tan \delta$ which provides information on the relationship between the elastic and

inelastic components. δ is phase lag between stress and strain's periodic wave (figure 1) and can determine the relationship between complex modulus(E*) and loss or storage modulus(E") as shown in the figure 1. If δ equals to 0 or 90 degree, the material is elastic or viscous, respectively. Moreover, the material should be viscoelasticity if δ is larger than 0 and less than 90 degrees. The objectives of most tissue research are viscoelastic and nearly incompressible materials. Therefore, the uniaxial tensile methodology is commonly applied in testing that uses a suitably shaped strip of specimen that is gripped at both ends by clamps and stretched while the load and extension are recorded [5-7].

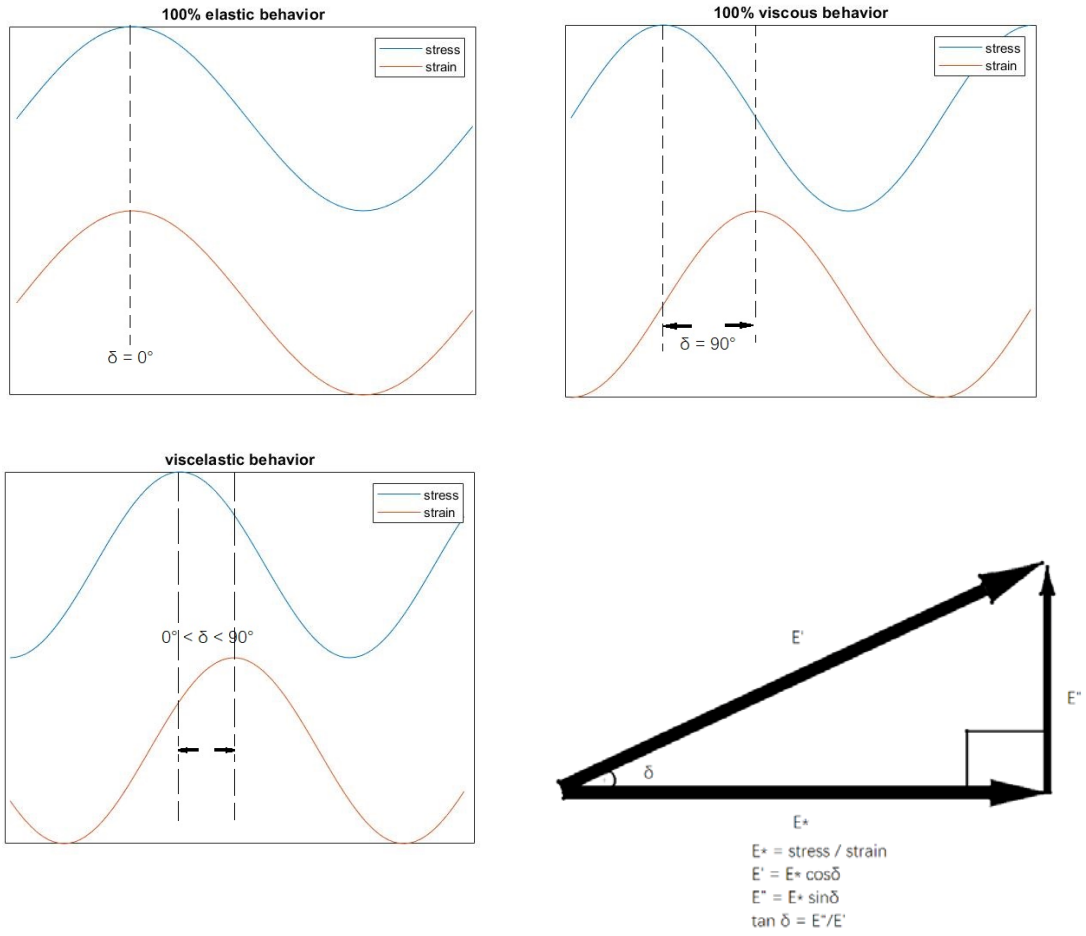

Figure 1 Relationship between stress and strain in a viscoelastic material

Palko et al (2011)[8] characterized the dynamic viscoelastic properties of canine sclera under cyclic strain input based on linear viscoelasticity and uniaxial tensile testing. Rectangular tissue strips cut by a custom made excision device with a gage width of approximately 3.7 mm and length of 16 mm were measured by electronic caliper which used a high frequency B-mode ultrasound prior to tissue dissection and the distance between the tissue grips was approximately 9.0 mm. The Rheometrics System Analyzer (RSA III, TA Instruments, New Castle, DE) was used to perform dynamic mechanical testing. They found that the data on the canine sclera was in good

agreement to the reported data on human sclera. In this study, little information is given on the grip method and clamp.

Oskui et al (2016)[9] focused on the dynamic tensile properties of the bovine periodontal ligament which has a non-linear strain-stress response. They confirmed that the properties are the function of loading frequency and preload. Additionally, the loading profile was chosen to be "force-controlled" rather than "displacement-controlled" in this study. The sample was bar-shaped parallel to the direction of mechanical testing with 4×8 mm dimensions and 2mm thickness which was measured by an optical microscope. A dynamic testing apparatus (TTDMA, Triton Technology, UK) was used to perform tensile test and a linear variable differential transformer (LVDT) was used to measure displacement. Apparatus clamps were used to hold the bone and tooth components and there is no other information about the clamp and gripping method. Finally, this study used a generalized Maxwell model that can capture the dependence of sample's viscoelastic behavior that was previously expressed by Gutierrez-Lemini (2014)[10] and Zhang and Gan (2014)[11]. The experimental results showed that the proposed model can be used in future finite element analysis and captured the viscoelastic behavior dependence on preload magnitudes.

Myers et al (2010)[12] tested both tensile and compression properties of soft tissue – human cervical tissue which is related to spontaneous preterm birth. They focused on the anisotropy effects by cutting tissue samples with three orthogonal axes and hypothesized that collagen orientation would influence the cervical tissue mechanical response. Additionally, a one-dimensional time-dependent rheological model was adopted to compare the samples with different

obstetric backgrounds, different anatomy sites and different loading direction. During the tension test, the dimension of the strip was approximately 2mm thick and had a 10mm gauge length. A universal material testing machine (Zwick Z2.5/TS1S, U1m, Germany) was used to performing mechanical test and all samples were bathed in PBS [13]. A video extensometer (Qimaging Retiga 1300 charge-couple device camera, 200 mm f/4 Nikon lens) and the CORRELATED SOLUTIONS VIC-2D version 4.4.0 software were used for capturing the transverse specimen deformation and lateral or axial stretch data. India ink were adopted to pattern the specimen and then stainless-steel tension grips with silicon carbide sandpaper and ethyl cyanoacrylate were used for gripping the sample. As a result, this study becomes a pioneer about characterizing the anisotropic nature of cervical tissue.

In vitro force-controlled method was adopted to perform the experiment by Boyce et al (2007)[14] which was similar to Oskui et al (2016)[9]. Bovine cornea has been tested to find out the viscoelastic response. Specifically, the loading can be divided into two types: cycled ramp test and multi-stress-rate cycles and a creep test which includes a range of hold stresses. The specimen size was 1.15-1.30mm thick and 7mm wide. The length ran from limbus and limbus and the gauge length is 8 mm. A servohydraulic load frame with pneumatically clamping serrated soft tissue grips and recirculated ophthalmic balanced saline solution bath was used to perform the tensile testing and immerse the tensile specimen and grips. This study compares the experimental results with a quasi-linear viscoelastic model and found that they were similar only when the stresses were low, and durations were moderate. Finally, the results of this study show significant non-linearity of bovine cornea and support the other studies of the stiffness of the tissue.

Huang et al (2009)[15] have studied the effect of temperature on the viscoelastic properties of the human supraspinatus tendon in tension. The specimen they used is a rectangular shape with the dimensions of 6.5 mm wide, 20 mm long and 1.5 mm thick which was cut by a sledge microtome (Leica Instruments, Nussloch, Germany) and measured by a stereomicroscope and a digital micrometer (Akizuki et al., 1986)[16]. The experiment was performed by a servo-hydraulic MTS machine (Model 858 Bionix, Eden Prairie, MN, USA) and adopted a static stress-relaxation method. Additionally, in order to prevent the specimen slippage, 400 grit sandpaper were applied to the clamp. Sub-failure material and viscoelasticity properties with quantified temperature were discussed in this study and thus give data that temperature effects should be considered as an important factor during the test.

Carlos et al (2005)[17] did three different tests of the human medial collateral ligament tissue which include a longitudinal test, a transverse test and a shear test and quantify the strain- and frequency-dependent viscoelastic behavior. The initial dimension of the medial collateral ligament test specimen before preconditioning was 12.9 mm long, 2.3 mm wide and 1.5 mm thick. A digital camera (Pulnix TM-1040, 1024x 1024x30 fps. Sunnyvale, CA) and frame-grabber (Bitflow Roadrunner, Woburn, MA) were used to record two black contrast makers which adhered to the longitudinal and transverse directions and a linear variable differential transformer (LVDT) (Schaevitz, Hampton, VA) was used to monitor the elongation. To prepare the specimen, hardened steel punches were adopted to harvest the test specimens. The results of this experiment indicated that the tissue is more effective at dissipating energy with higher frequencies at fasting loading rates.

2.2 Motivation

However, in the last few years, there has been interest in the study of shoulder joint which made up of the humerus, collarbone and scapula, in which there are a lot of ligaments, muscles and soft tissues. However, when compared with other joints, the shoulder joint is even more fragile because necessity of the arm motion in all direction, thus there is very little bone support in the joint and soft tissue controls much of the motion. For this reason, the shoulder can get injured due to excessive force or non-standard movement.

2.3 Mechanics of shoulder joint

"The shoulder joint is one of the most mobile in the body, at the expense of stability."[18] The bones of the shoulder joint are composed of the humerus, the scapula and the clavicle. The scapula and clavicle are located at the top of the chest and many upper back and shoulder muscles are to attach the scapula in the upper back and the clavicle in the upper thorax to the chest and spine. This provides a platform for arm and shoulder movement. The shoulder joint is a ball and socket joint consisting of the humeral head and the joint socket (glenoid), which forms the bony articulation. This joint has the most motion of any joint in the body. The upward movement of the humerus is blocked by the condyles of the clavicle and shoulder blades, as well as the ligaments and rotator cuffs. The downward, forward, and backward movement of the humerus is limited by the position of the humeral head in the labrum of the glenoid, which is an annular band of fibrocartilage that wraps around the edge of the socket to add concavity. The humerus is fixed by

many of ligaments and tendons which include glenohumeral ligament along the labrum. These ligaments and tendons form the rotator cuff.

If the muscle or ligament, or any of the soft tissues are injured, then scapula will lose control and then the shoulder joint may have impingement syndrome or other damage. The ligaments, especially the glenohumeral ligament, play a key role in stabilizing the bony structures. The anatomy of shoulder joint is shown in the figure 2. The glenohumeral ligament connects the humerus with the glenoid fossa and is main structure in maintaining the stability and preventing dislocation.

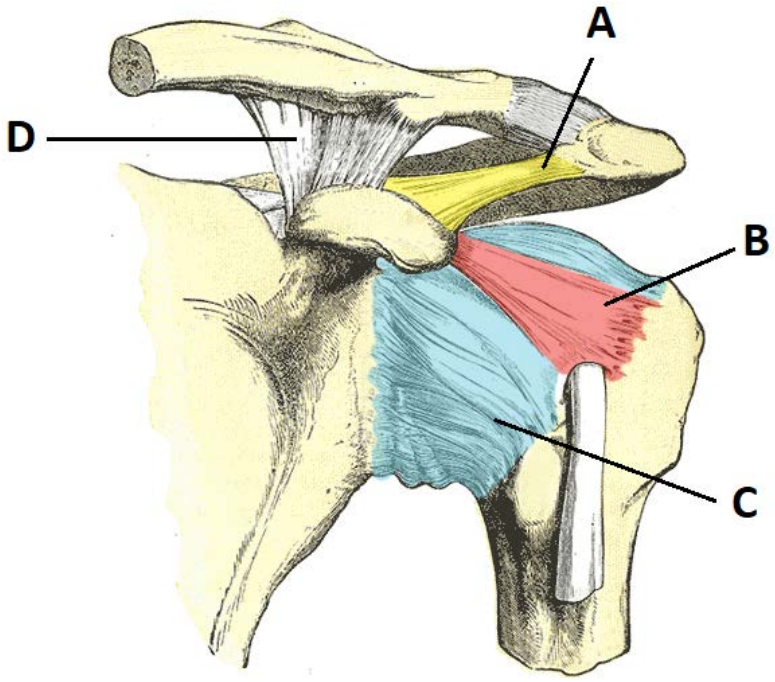

Figure 2 The structure of the shoulder joint A-Coracoacromial ligament B-Coracohumeral ligament C-Glenohumeral ligaments[18]

2.4 **Study of the glenohumeral ligament**

Among early studies, Bigliani et al (1992)[19] discussed the properties of the inferior glenohumeral ligament, especially the tensile property, and the influence of the tissue structure. Since the torsion of the shoulder is limited by the flexibility of the ligament, the scale of the external torsion is limited by the stiffness of the inferior glenohumeral ligament and the tightness of the upper part of the capsular ligament. It is necessary to add an abduction angle to the inferior glenohumeral ligament when studying the tensile properties of the tissue. Therefore, this study had divided the inferior glenohumeral ligament into three parts with different angles. In this study, the author investigates the properties of elongation rate, failure stresses and failure strains, failure modes and tensile modulus and the stress-strain relationship. The dimension of specimens used were measured by a Bausch and Lomb stereo-zoom microscope, adapted with an Olympus precision X-Y translation stage, Leitz electrooptical micrometer coupled to a Microcode digital micrometer. The mean length, width and thickness are nearly 40mm, 12mm and 2mm, respectively. During tensile testing, video dimensional analysis was used to track the changes in gauge section length electronically. Finally, this study found a great influence of the degree to which capsular stretching can take place in the production of traumatic glenohumeral instability.

Ticker et al (1996)[20] analyzed the geometric and strain-rate dependent properties of the inferior glenohumeral ligament (IGHL). The sacral ligament is the most important static factor for stabilizing the shoulder joint. In this experiment, a materials testing machine and 3D software were used to analyze the length changes of the ligament and grip-to-grip displacements during normal human shoulder abduction. The mean dimension of these samples is 43mm in length, 1.9 mm in thickness, and 13.6mm in width. The results of the study have significance for the clinical treatment of shoulder joint disease. The IGHL is not in a state of tension during the initial stages

of outreach and becomes tenser as the angle of outreach increases. Therefore, this study only focused on the IGHL at its maximum length and its position on the surface of the humeral head at this time.

In addition, Lee et al (1999)[21] focused on the structural properties of the glenoid with or without anterior band of the inferior glenohumeral ligament with and without humerus complex. Both a younger group and an older group were introduced for the process of evaluating the biomechanical properties with age. The purpose of this study was to compare bio-mechanical properties of the glenoid with or without anterior band of the inferior glenohumeral ligament with and without humerus complex in the apprehension position by different age groups. Tensile testing was conducted by adopting a video digitizing system. The maximum and the minimum of the sample width was 29.7mm and 22.3mm and the thickness of all was above 3mm. An axial testing machine (Instron Co., Canton, MA, USA) was used to perform the dynamic test and a custom shoulder jig and a video digitizing system (VDS) is used to measure the strain. The results were divided into three main parts, namely, geometric properties, failure characteristics, and bio-mechanical properties. It was found that as to the structural properties, the older group has more volume and cross-area than the younger group. The results of this article stated that for these individuals who are very young, disruption of the complex usually can be found at the glenoid insertion site, but for older individuals, disruption has a great chance to take place at the midsubstance region. Overall, this article finds the conclusion that as to the structural properties and the material characteristics of the inferior glenohumeral ligament, the younger group is significantly different with the older group and the younger group is more superior.

Pollock et al. (2000)[22] looked at the effect of repetitive subfailure strains on the inferior glenohumeral ligament. This experiment was divided into three groups with the only difference

between each group being the number of cycles of subfailure strain after applied a 1.5-N preload to establish its initial length. A servo-hydraulic and axial/torsional testing system (MTS Systems Corporation, Minneapolis, Minn) was used performed the test. It was noted that when gripping the samples, the sample need to be carefully aligned in the testing apparatus with the uniaxial tensile loading direction conforming to the predominant fiber orientation. Finally, specimens were in a lax state for 15 minutes and conditioned for 30 cycles of L1 strain. Then, after maintained in a lax state for an additional 45 minutes, the samples were conditioned for another 30 cycles of L1 strain, thus giving seven loading segments like shown in figure 3. Overall, this article demonstrates the hypnosis that cumulative injury such as repeated subfailure strain of IGHL will lead to irreversible damage.

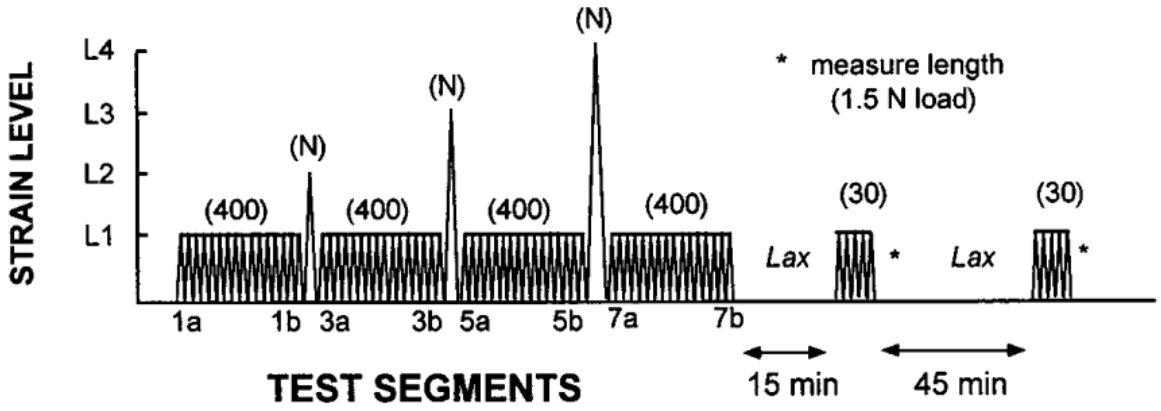

Figure 3 Testing protocol [22]

Finally, based on the based on the previous studies of the glenohumeral ligament, it is easy to find that there are still some gaps in the current research. For example, there is a need to study the mechanical properties of small tissue samples from different regions of the rotator cuff.

Therefore, in my study, the goal is to investigate materials and methods for testing small tissue samples.

3.0 Methods

3.1 Test machine and clamps

This study is designed to use the DMA Q800 testing machine (DMA, Q800, TA Instruments) (Figure 5) which is a dynamic mechanical analyzer that induces either oscillatory deformation, oscillatory force, static deformation or static force to produce a stress response of the materials. In a tensile test, the sample are to be placed between a fixed clamp and a movable clamp while a measured force is applied in by a displacement of the moving clamp. An optical encoder is used to measure the clamp displacement which has a maximum value of 25 mm. According to the DMA theory, optical encoders provide 1 nanometer resolution of displacement which based on the diffraction patterns of light which shows in figure below. Some of necessary equations used here are the definition of strain and stress and the simplest of stress/strain law , Hooke's law, which is shown below. In these equations, ΔL and A are the change length of the gauge length and cross-sectional area of gauge area, respectively, rather than the total displacement of the cross-head which may include specimen slip. By St. Venant's Principle, which means when far enough away from the load's point of application, it can be assume the stress is uniform for equivalent loads, only the gauge length area needs to be analyzed. Thus, it is only necessary to determine the elongation of gauge length. Finally, the applied force and deflection can be translated into strain-stress curve which can extract a variety of tensile properties[23]-[24].

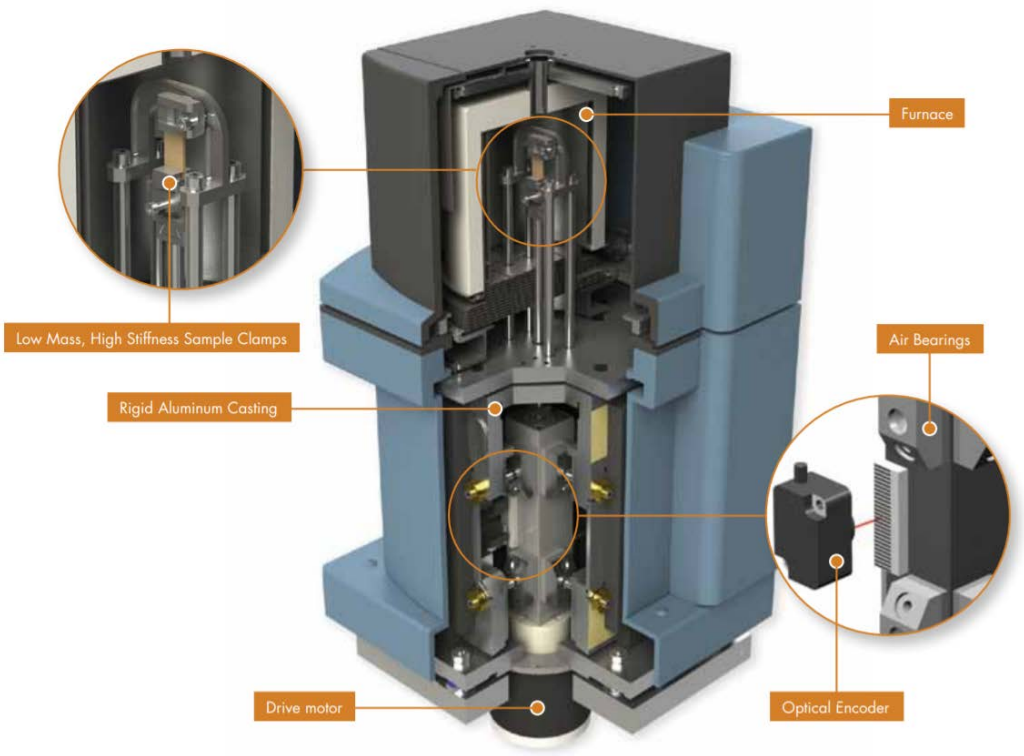

Figure 4 Structure of DMA Q800[25]

$$\varepsilon_x = \frac{\Delta L}{L} \tag{1}$$

$$\sigma_x = \frac{F}{A} \tag{2}$$

$$\sigma_x = E\,\varepsilon_x \tag{3}$$

ε_x——strain in the x direction

ΔL——displacement

σ_x——stress in the x direction

A ——cross-section area

E ——elasticity modulus

The DMA Q800 has many types of fixtures which can allow different loading such as dual/single cantilever, 3-point bending, shear sandwich, compression, tension, and submersible clamps. One of the goals of this study was to design a set of clamps that could be used for tensile testing. However, the clamp should be designed for the testing of small tissue samples. The dimension of custom-designed tension clamp is shown in figure 5 and the finished clamp is shown in figure 8. The round washer attached to the movable clamp are used to connect the movable grip with the movable bar support and the total travel length is 25 mm. The vital thing that during the design is concerning the distance between the movable grip and stationary grip which related to the length of the specimen and the travel length of the movable support. The specific designed clamp dimensions are shown in figure 6 which is fixed clamp and figure 7 which is movable clamp.

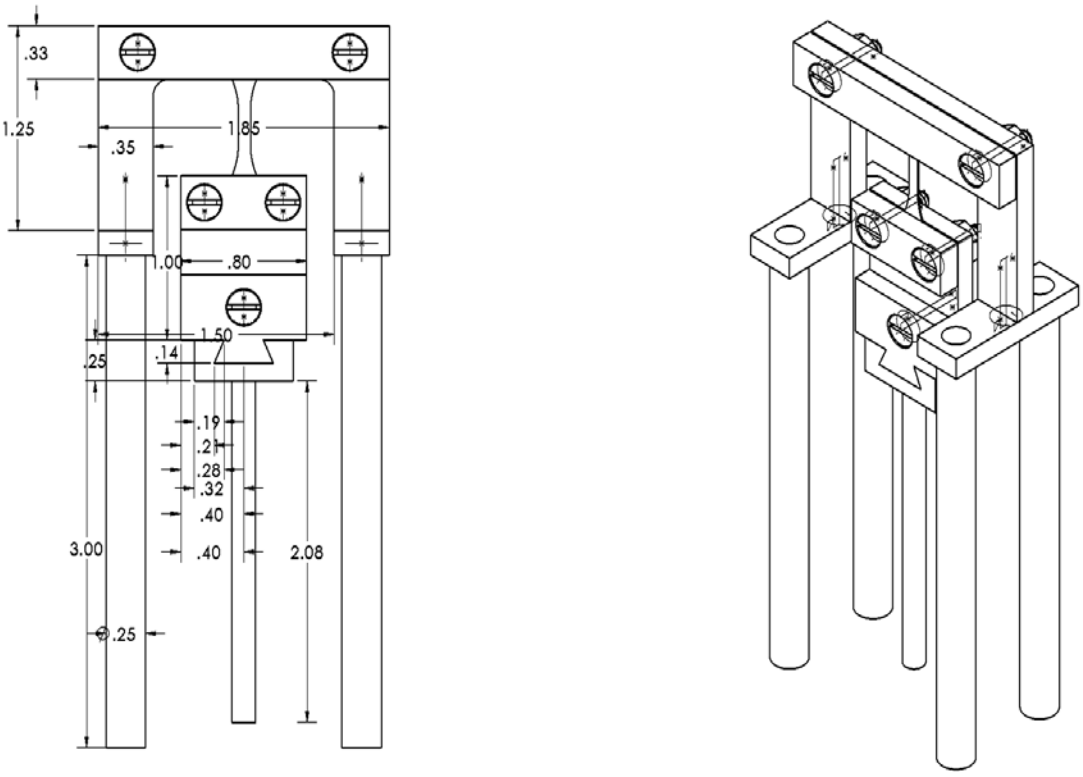

Figure 5 Dimension of mounted clamp in machine

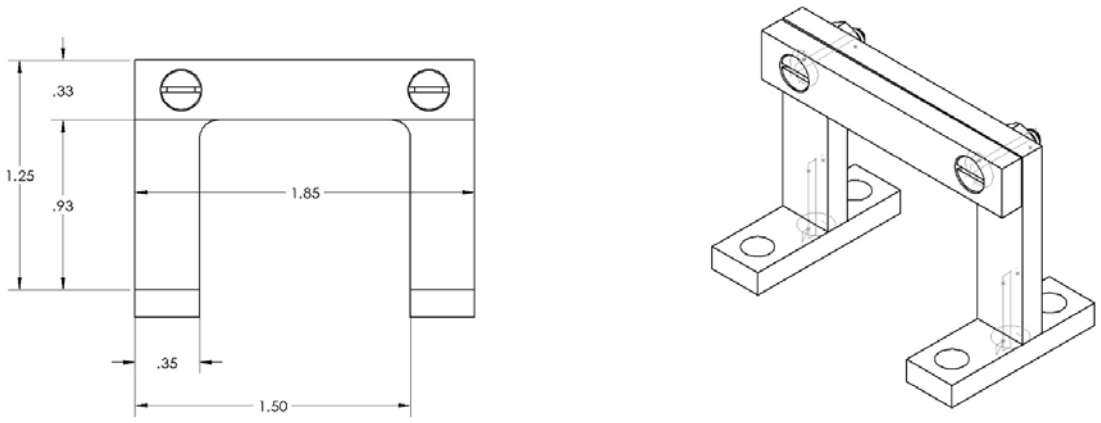

Figure 6 Fixed clamp

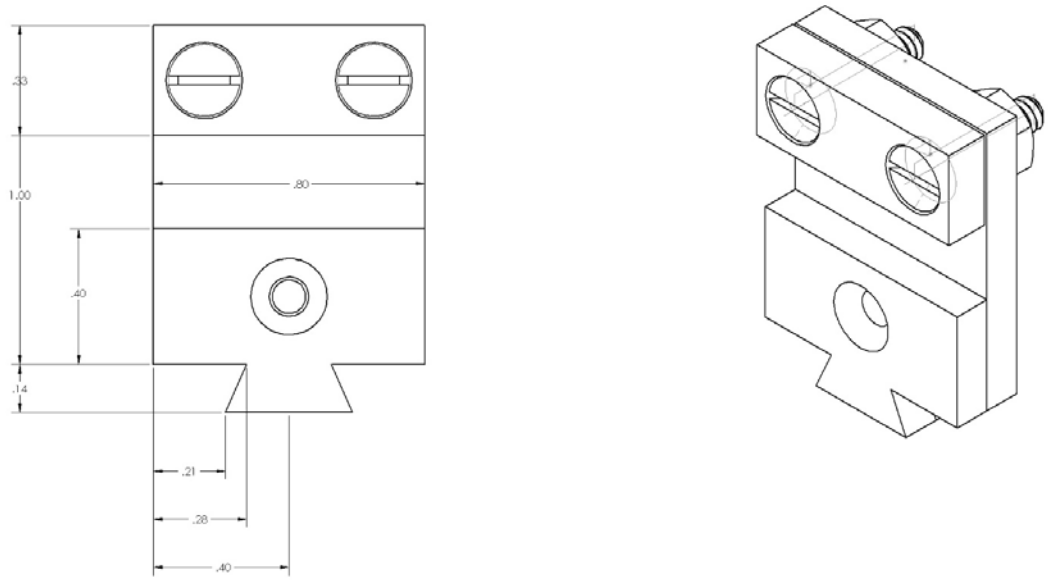

Figure 7 Movable clamp

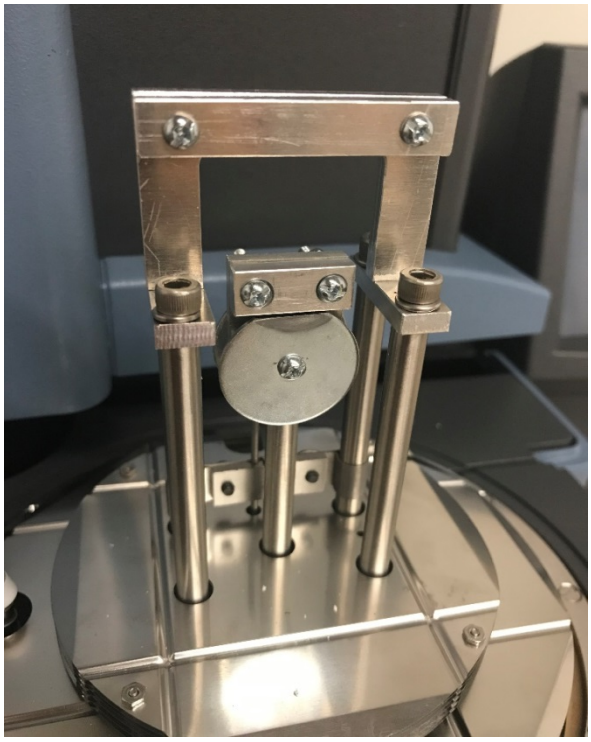

Figure 8 Tension clamp

3.2 Test specimen geometry

Many reasons can lead to sample buckling during tension testing such as non-uniform loading or non-axial loading. If the sample buckles or is non-uniformly strained during loading, this will lead to errors in the measurement of properties. To prevent this, it is necessary to use a specimen shape which will have a region of uniform tension. For this reason, most tensile specimen shapes use an hourglass shape, sometimes known as a dog bone, with a standardized geometry. While there are standardized shapes are for larger specimens, however, this study wanted to use the smallest possible specimen, so part of this study was to design specimen test geometry and fabricate a die to cut this shape.

In designing a specimen shape for this study, the first thing is to review current standardized shapes. The most common of the mechanical tests is tensile test and is described in detail in many standards. A dog bone or dumbbell type specimen is machined or punched out and the specimen can be made from a sheet or plate of metal or plastic. The American Society for Testing and Materials (ASTM) and the International Organization for Standardization (ISO) have some different standards for tensile specimens and these will be reviewed. The most significant differences between each standard are applicable materials and standard dimensions and most have nearly the same shape - a dumbbell shape. This geometry allows the specimen to be gripped and loaded without failure in the gripping region, while having deformation and failure confined to a narrow central gauge section [26]. These different grips will be compared in selecting geometry for the shape of the small test specimen.

The ASTM D638 geometry [27], which is mainly used to test the tensile properties of plastic materials, is applicable for test samples of any thickness up to 14 mm and no less than 1 mm. There are five sizes of the geometry that used for different thicknesses. Because the desired specimen size is small, type 5 (figure 9) and type 4 (figure 10), which are used for thin plastic materials, will be considered. However, a short coming of this model is that the test region is short when compared with the grip section and thus the relative specimen length is large. Table 1 and table 2 in appendix A show the dimension of this standard.

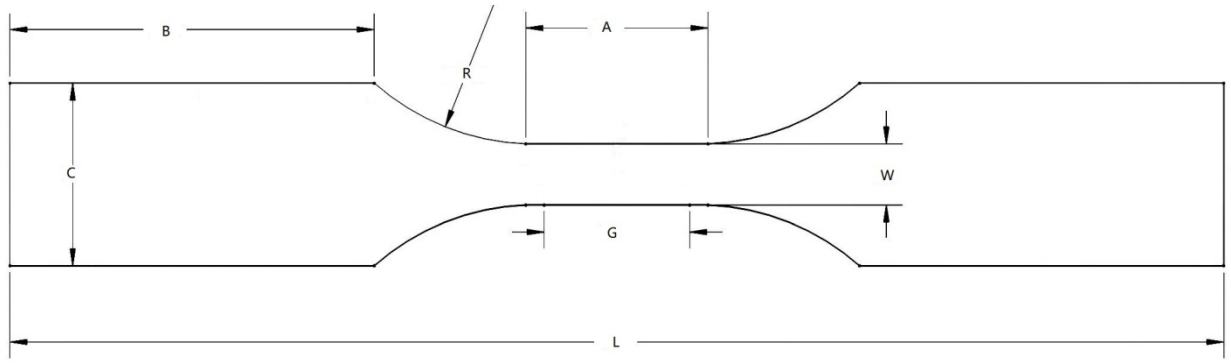

Figure 9 Type 5 of ASTM A638

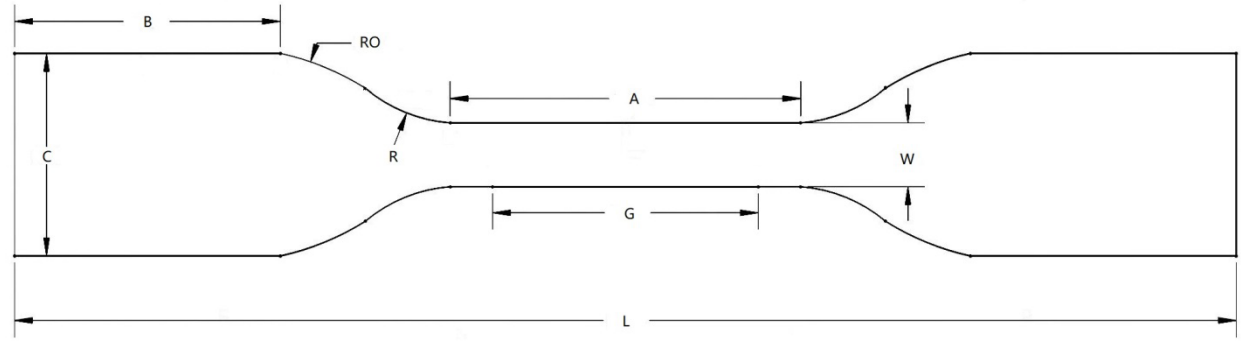

Figure 10 Type 4 of ASTM A638

The dimensions of specimens ASTM A370[28] and ASTM E8[29] are very close. E8/E8M and A370 are primarily used for metallic materials and steels. In this model, the cross-sectional area at the center of the sample is the smallest to ensure that fracture occurs within the gauge length. The shape of this model is given in figure 11 and has a long grip area so that the overall specimen length is relatively long. This is a disadvantage to having a small specimen size as desired for this study. Table 1 summarizes the dimensions of some of the standard test specimen geometries and table 3 in appendix A has gathered the full dimension of each standard.

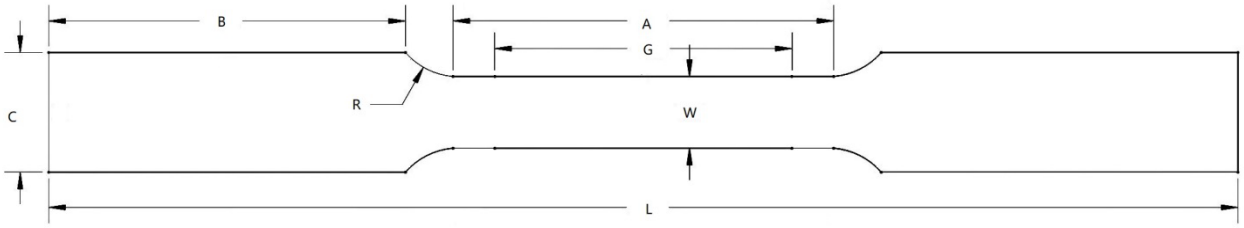

Figure 11 ASTM E8

ISO 527[30] is another standard that gives tensile sample geometry (Figure 12). This geometry is typically used for rigid and semi-rigid thermoplastics moldings, extrusion and cast materials. Because of the small grip region, the relative length of the geometry is smaller and therefore may be suitable for small tissue samples. The dimension can be seen in table 1 and appendix table 4.

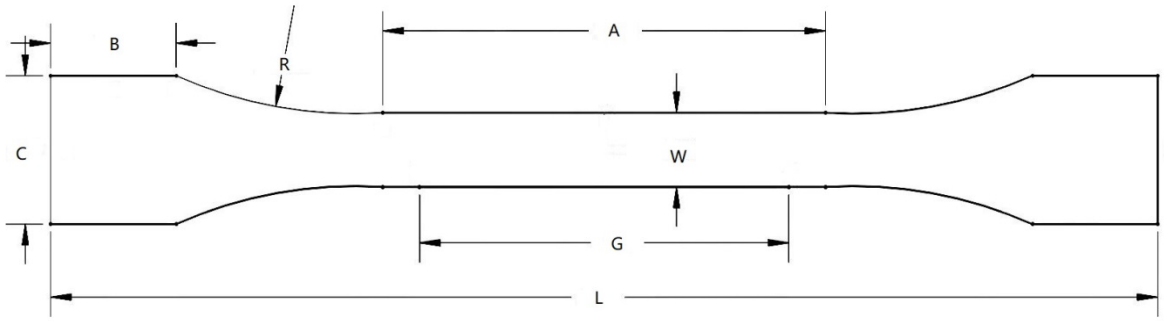

Figure 12 ISO 527

There many other standards that specify dimensions of tensile samples. Some of these are ISO 37 which is applicable for rubber, vulcanized or thermoplastic, ASTM D412 for vulcanized rubber and thermoplastic elastomers and other additional standard tests used for film like ASTM D88-10, JIS K7172 and others. Since it is desired to have a small soft tissue, the standard geometry will be scaled down to widths of 1 mm, 2 mm and 3 mm which shows in appendix A. Appendix

A shows the E8, ISO 527 and D638 standards suggested sizes after scaling down. The part of compared table 1 and the cutting die which made by additive manufacturing machine are showing in figure 13. In this study, the shape of the specimen were based on ISO 527 because the gauge section is long enough to analysis and grip section is large enough to avoid slippery with the friction of sandpaper. Additionally, when comparing 1 mm, 2 mm, and 3 mm width of ISO 527 shape, it is suitable for experiment to adopt 1 mm width because of the small geometry of glenohumeral ligament.

Table 1 The dimensions of different tensile specimen geometry

	E8/E8M	ISO 527	D638 type 5		type 4
G-gauge length	4.17	5.00	2.40	G-gauge length	4.17
W-width	1.00	1.00	1.00	W-width	1.00
R-radius of fillet	1.00	6.00	3.99	R-radius of fillet	2.33
L-overall length	16.67	15.00	19.97	L-overall length	19.17
A-length of reduced parallel section	5.33	6.00	3.00	A-length of reduced parallel section	5.50
B-length of grip section	5.00	1.70	5.99	B-length of grip section	4.17
C-width of grip section	1.67	2.00	3.00	C-width of grip section	3.17
				RO-outer radius	4.17

Figure 13 Cutting die

3.3 Sample preparation

Chicken skin and leg tendon were used to test the performance of the punch. During cutting the samples, the punch is used to cut the chicken skin and tendon in order to prepare the tensile strip. However, when consider the multilayer of the skin and the viscoelasticity of the tendon, it was difficult to cut the sample only with the use of the punch. Thus, a shape precision knife and blades are important auxiliary means. The punch was first been put down on the tissue to leave an outline of the tensile strip shape and then the knife was cutting along with the outline. The cut tissue samples are shown in figure 14 and 15.

Figure 14 Sample cut from chicken tendon

Figure 15 Samples cut from chicken skin

4.0 Finite element analysis

Finite element analysis is a widely used numerical method which can solved complex structure problems accurately. It divides a complex structure into many smaller pieces that can be solved easier and finally obtain the overall solution.

The two-dimensional model of the designed tensile sample geometry, with the dimensions given in table 1 -- ISO 527, which is the same like the punch and the specimen shape, is shown in figure 14. In this case, the material is a linear elastic isotropic solid and the Poisson's ratio and elasticity modulus are 0.49 and $3\times10^{\wedge4}$ psi, respectively, and the length of each element edge is 0.1. The displacement of the top griped section is zero in x-direction and y-direction. However, the displacement of the bottom gripped section is zero in x-direction and has a 5% elongation of the total length which is 0.75 mm in y-direction. For simulating the real experiment, there are must some area which have been gripped. Thus, it is assumed that the clamps have gripped half of the grip area without any slippage during elongation and the boundary conditions and the material properties are the same. The finite element model of the specimen is shown in figure 16.

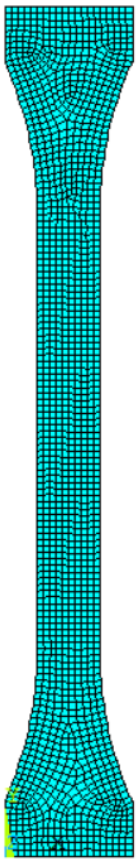

Figure 16 Finite element model of the specimen

5.0 Results

After setting the boundary conditions, the deformed shape shows in figure 17 and the black dotted line in this figure is undeformed shape edge. It is obvious that the model has been stretching.

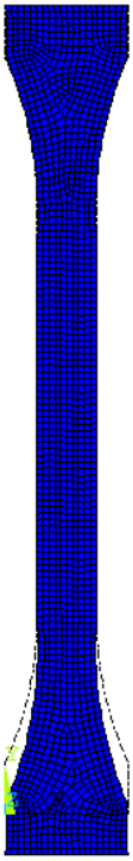

Figure 17 Finite element result showing the deformed shape with undeformed edge

5.1 **Contour plot of finite element analysis**

The figures shows below are stress distributions for σ_{xx}, σ_{yy} and shear stress. All the figures are nodal solution which is more precise than the element solution. It can be easily seen that the stress distributions in gauge length area are nearly become uniform in all direction because of the Saint Venant's Principle which means the external force only influence the stress distribution near the force area. Like the problem in this model, the gauge area is far enough from the gripped area which is also applied force in y-direction. Thus, the maximum stress σ_{yy} occurred at the gripped area and the stress becomes uniform when getting far from the gripped area. The stress distribution of σ_{xx} is small because we only applied the force in y-direction. Additionally, all of the loads are vertical to the bottom surface. Thus, in this situation, the normal stress is much larger and more significant in analyzing the solid instead of shear stress. Thus, we only need to consider the normal stress which means σ_{xx} and σ_{yy}, especially σ_{yy}.

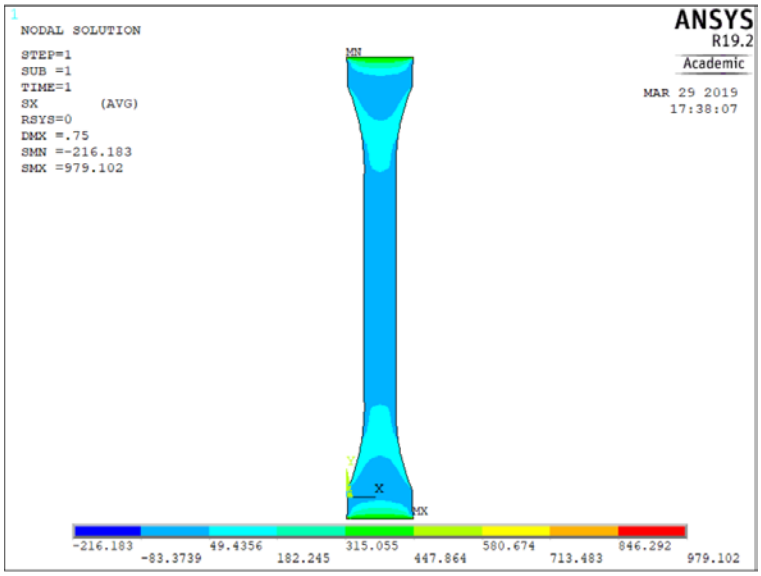

Figure 18 σ_{xx} distribution

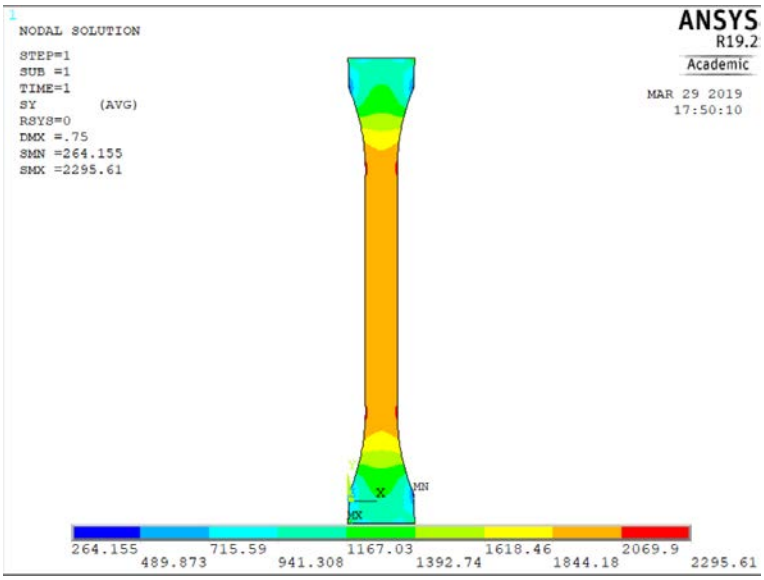

Figure 19 σ_{yy} distribution

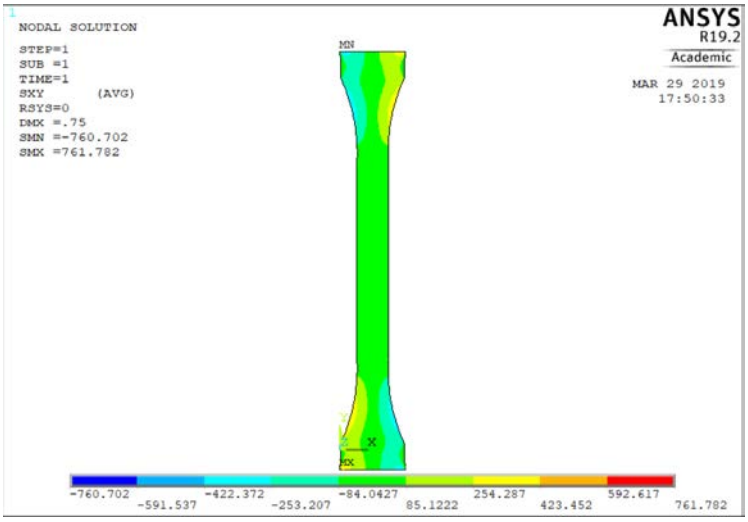

Figure 20 σ_{xy} distribution

5.2 **Path plot of finite element analysis**

To investigate the stress distribution in greater detail, stress will be plotted along horizontal sections across the top, middle and bottom of the model(figure 21), which represent different situation in tension strip during the stretch. By this method, the stress change in the tissue is more clearly and straightforward for further analysis.

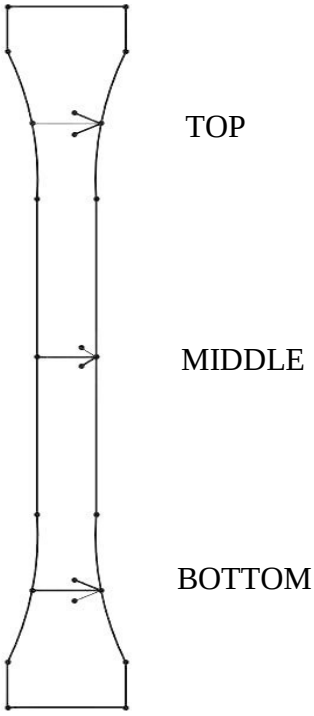

Figure 21 Position of top, middle and bottom location of the stress plots

5.2.1 Stress path plot of σ_{xx}

From the figures showed above, two cases are nearly the same no matter the trend and the data, and the trends agree with the trend in contour plot. However, the path plot of the middle of the tissue is different from the contour plot which is uniform. There are three reasons. First, after looking carefully of the data in the diagram, the differences of maximum value and minimum value in in figure 23 are small when compared with the differences in figure 22 and 24. Second, the gauge length is not long enough for the stress to become uniform.in Saint Venant's principle, an important condition is the distance is long enough away from the force area. And finally, the direction of the applied force is different with x-direction.

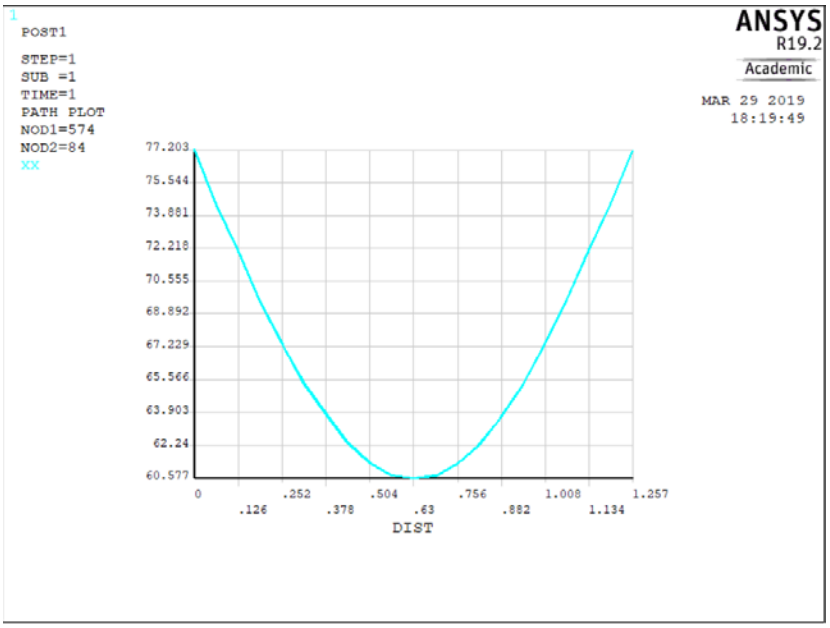

Figure 22 Top path of σ_{xx}

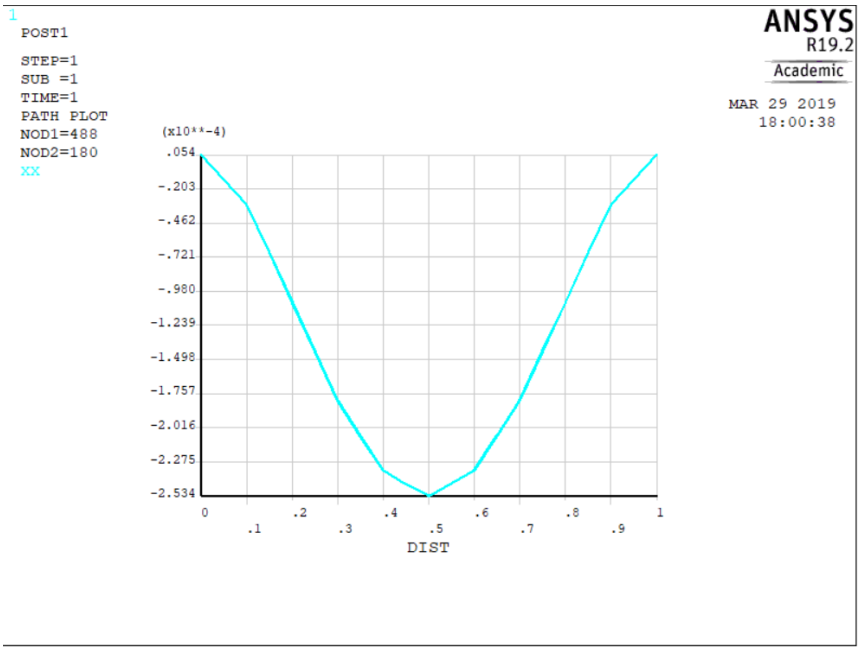

Figure 23 Middle path of σ_{xx}

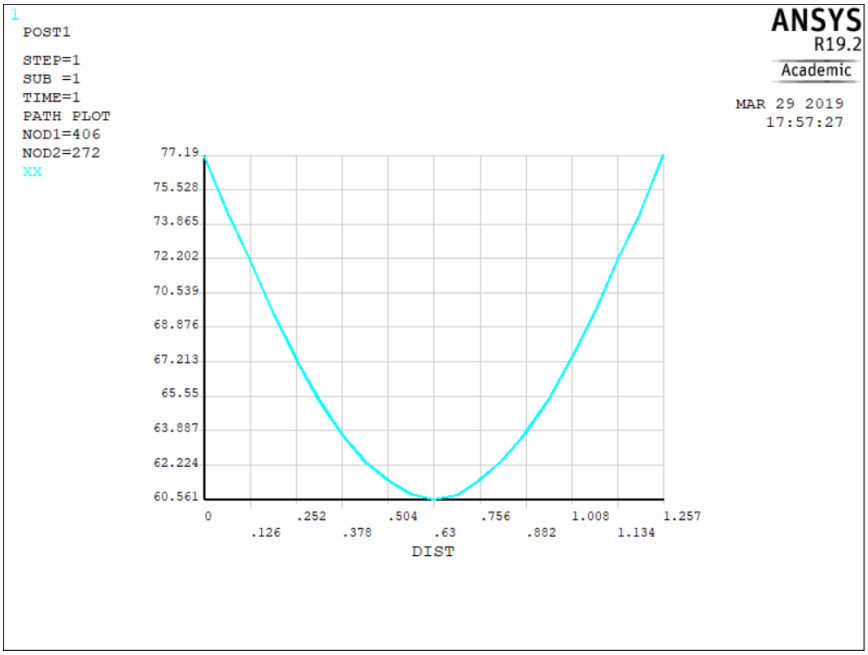

Figure 24 Bottom path of σ_{xx}

5.2.2 Stress path plot of σ_{yy}

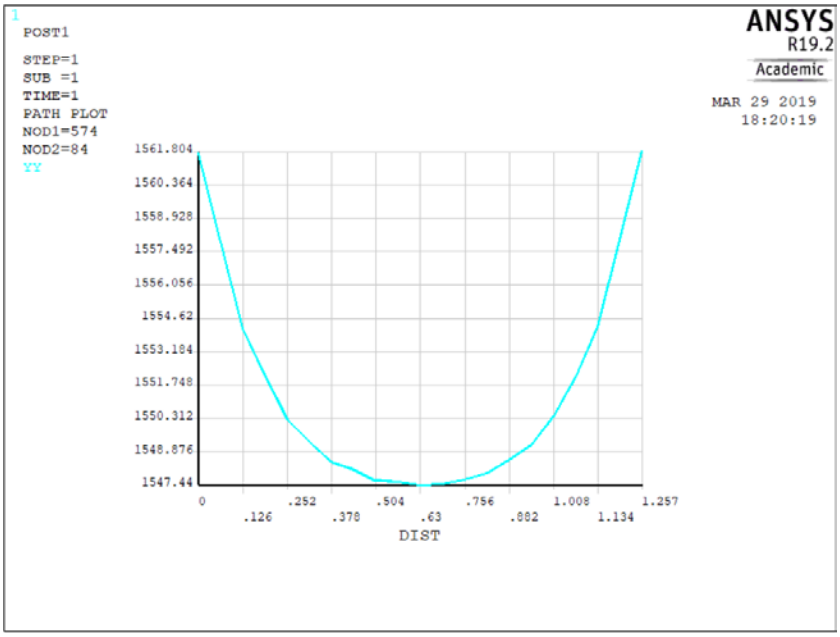

Figure 25 Top path of σ_{yy}

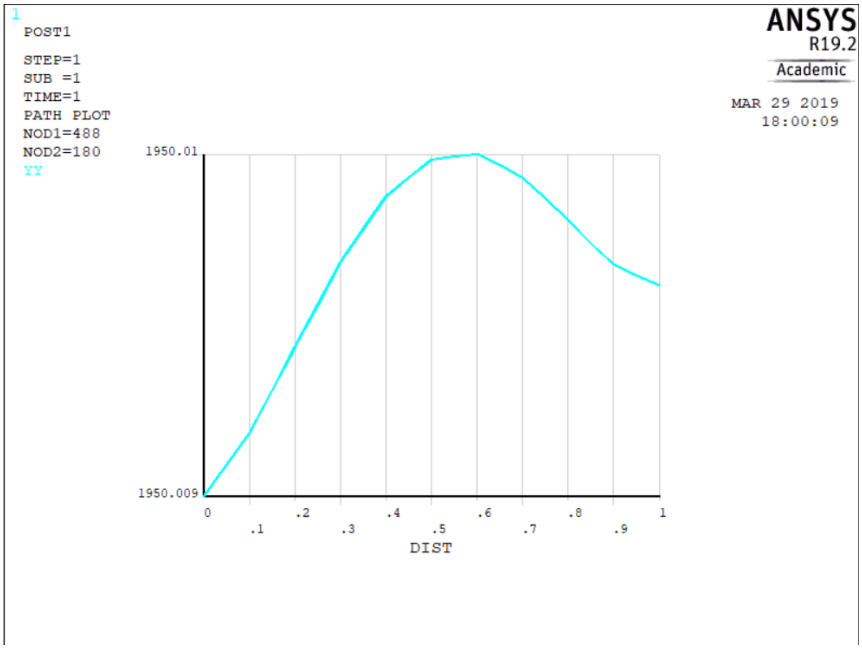

Figure 26 Middle path of σ_{yy}

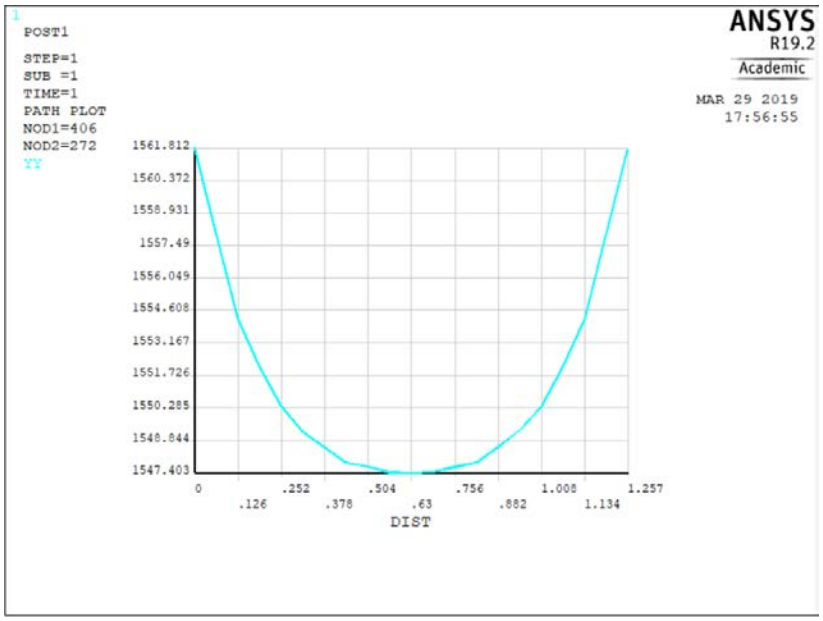

Figure 27 Bottom path of σ_{yy}

The stress of σ_{yy} is important and large because the direction of the applied force is align with y-direction. The trend and the data are nearly the same with the contour plot. Moreover, the stress in middle of the tissue is almost become uniform with little difference which can be ignore. This situation is in agreement with Saint Vanant's principle and contour plot.

5.2.3 Shear stress path plot

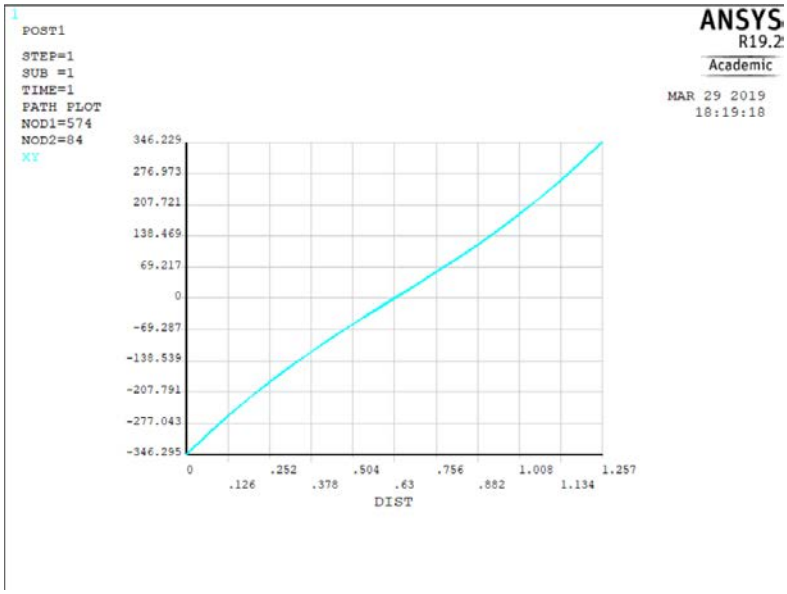

Figure 28 Top path of σ_{xy}

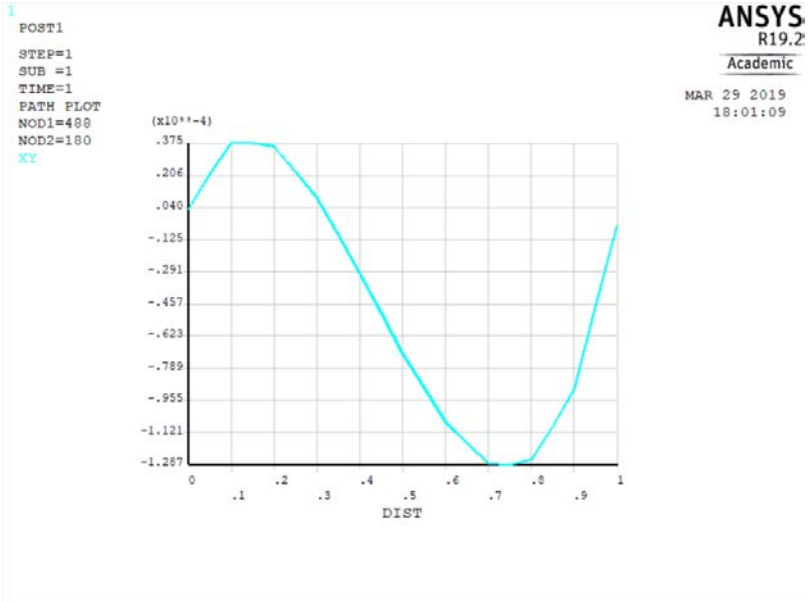

Figure 29 Middle path of σ_{xy}

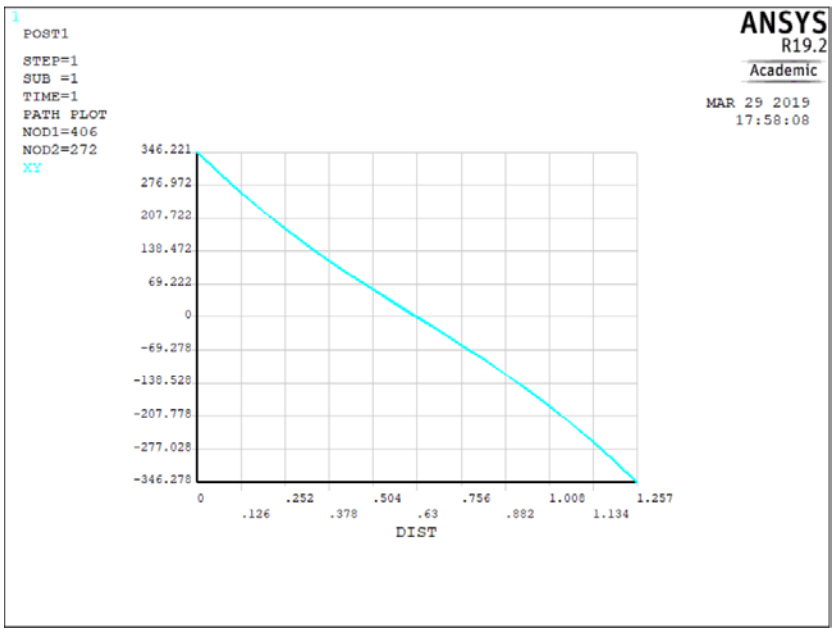

Figure 30 Bottom path of σ_{xy}

The shear stress in the middle section (figure 29) is very small and skew symmetric which can be ignore. This data proves that the shear stress in this situation is less significant. In other figures which near the grip section, the shear stress is large. Additionally, from what can be seeing above, figure 28 and 30 is also skew symmetric, so as to figure 29. Therefore, the shear stress in the tissue is nearly skew symmetric which is the same as what can be seen in the contour plot.

6.0 Discussion

The stress analysis for the glenohumeral ligament in shoulder joint was explored using finite element analysis and the specimen was cutting from the shoulder joint by adopt a standard custom-made punch. Additionally, a custom-made clamp was also been designed for further experiment.

During cutting samples, the main issue and the initial difficulty came from the fact that it was skin that being punched out first. Because the multilayer of the skin, it is difficult to cut a precise standard size of the tension trip. Thus, we tried on the tendon and ligament which is much easier to punched out. Even still, the samples from both skin or ligament is turned out to be shapely enough to be test with the help of a more precision knife. Going forward, the punch method will work well.

Therefore, An axisymmetric finite element model of the glenohumeral ligament strip was constructed in terms of the known geometries and material properties. The properties of the tissue were chosen to be linear elastic based on properties available in the literature. The results in chapter 5 proves that the ISO 527 standard geometry can be used in the further experiment. Additionally, the dumbbell shape of tension strip is necessary for the experiment because this shape decrease the influence of slippery, shape and the unequal force applied on the tissue.

Finally, because of the lack of the materials constants, one limitation of the model is the linear elastic properties used for the tissue. Experimental characterizations of the material constants for the glenohumeral ligament would be very advantageous in using finite element analysis, and moreover, can prove the results of the finite element analysis.

Appendix A Dimensions of each standards

When design the clamps, many standard was taken into account and scale down with 1 mm, 2 mm and 3 mm width of gauge length. The dimensions were shown in table 2 to 5.

Table 2 Different sizes of E8/E8M geometry

E8/E8M(mm)			
G-gauge length	4.17	8.33	12.50
W-width	1.00	2.00	3.00
R-radius of fillet	1.00	2.00	3.00
L-overall length	16.67	33.33	50.00
A-length of reduced parallel section	5.33	10.67	16.00
B-length of grip section	5.00	10.00	15.00
C-width of grip section	1.67	3.33	5.00

Table 3 Different sizes of ISO 527 geometry

ISO 527-2(mm)			
G-gauge length	5.00	10.00	15.00
W-width	1.00	2.00	3.00
R-radius of fillet	6.00	12.00	18.00
L-overall length	15.00	30.00	45.00
A-length of reduced parallel section	6.00	12.00	18.00
B-length of grip section	1.70	3.40	5.10
C-width of grip section	2.00	4.00	6.00

Table 4 Different sizes of D638 type 5 geometry

D638(mm)			
type 5			
G-gauge length	2.40	4.79	7.19
W-width	1.00	2.00	3.00
R-radius of fillet	3.99	7.99	11.98
L-overall length	19.97	39.94	59.91
A-length of reduced parallel section	3.00	5.99	8.99
B-length of grip section	5.99	11.98	17.97
C-width of grip section	3.00	5.99	8.99

Table 5 Different sizes of D638 type 4 geometry

type 4			
G-gauge length	4.17	8.33	12.50
W-width	1.00	2.00	3.00
R-radius of fillet	2.33	4.67	7.00
L-overall length	19.17	38.33	57.50
A-length of reduced parallel section	5.50	11.00	16.50
B-length of grip section	4.17	8.33	12.50
C-width of grip section	3.17	6.33	9.50
RO-outer radius	4.17	8.33	12.50

Bibliography

[1] M.M. Verver, J. van Hoof, C.W.J. Oomens, J.S.H.M. Wismans & F.P.T. Baaijens (2004) A Finite Element Model of the Human Buttocks for Prediction of Seat Pressure Distributions, Computer Methods in Biomechanics and Biomedical Engineering, 7:4, 193-203, DOI: 10.1080/10255840410001727832

[2] M. Komljenović, Mechanical strength and Young's modulus of alkali-activated cement-based binders, Editor(s): F. Pacheco-Torgal, J.A. Labrincha, C. Leonelli, A. Palomo, P. Chindaprasirt, Handbook of Alkali-Activated Cements, Mortars and Concretes, Woodhead Publishing, 2015, Pages 171-215, ISBN 9781782422761,

[3] Chan BP, Leong KW. Scaffolding in tissue engineering: general approaches and tissue-specific considerations. Eur Spine J. 2008;17:467–479.

[4] Nimeskern L, van Osch GJ, Müller R, Stok KS. Quantitative evaluation of mechanical properties in tissue-engineered auricular cartilage. Tissue Eng Part B Rev. 2014;20:17–27.

[5] Ní Annaidh A, Bruyère K, Destrade M, Gilchrist MD, Otténio M. Characterization of the anisotropic mechanical properties of excised human skin. J Mech Behav Biomed Mater. 2012;5:139–148.

[6] Ottenio M, Tran D, Ní Annaidh A, Gilchrist MD, Bruyère K. Strain rate and anisotropy effects on the tensile failure characteristics of human skin. J Mech Behav Biomed Mater. 2015;41:241–250.

[7] Hussain SH, Limthongkul B, Humphreys TR. The biomechanical properties of the skin. Dermatol Surg. 2013;39:193–203.

[8] Joel R. Palko, Xueliang Pan, Jun Liu, Dynamic testing of regional viscoelastic behavior of canine sclera, Experimental Eye Research, Volume 93, Issue 6, 2011, Pages 825-832, ISSN 0014-4835.

[9] Iman Z. Oskui, Ata Hashemi, Dynamic tensile properties of bovine periodontal ligament: A nonlinear viscoelastic model, Journal of Biomechanics, Volume 49, Issue 5, 2016, Pages 756-764, ISSN 0021-9290.

[10] Gutierrez-Lemini, D., 2014. Engineering viscoelasticity. Springer, New York, pp. 93-112

[11] Zhang, X., Gan, R.Z., 2014. Dynamic properties of human stapedial annular ligament measured with frequency-temperature superposition. J. Biomecha. Eng. 136, 081004

[12] Myers KM, Socrate S, Paskaleva A, House M. A Study of the Anisotropy and Tension/Compression Behavior of Human Cervical Tissue. ASME. J Biomech Eng. 2010;132(2):021003-021003-15. doi:10.1115/1.3197847.

[13] Myers, K. M., Socrate, S., Tzeranis, D., and House, M. D., 2009, "Changes in the Biochemical Constituents and Morphologic Appearance of the Human Cervical Stroma During Pregnancy," Eur. J. Obstet. Gynecol. Reprod. Biol., 144, pp. S82–S89.

[14] Boyce, B. L. , Jones, R. E. , Nguyen, T. D. , & Grazier, J. M. . (2007). Stress-controlled viscoelastic tensile response of bovine cornea. Journal of Biomechanics, 40(11), 2367-2376.,

[15] Huang, C. Y. , Wang, V. M. , Flatow, E. L. , & Mow, V. C. . (2009). Temperature-dependent viscoelastic properties of the human supraspinatus tendon. *Journal of Biomechanics, 42*(4), 546-549.

[16] Akizuki, S., mow., Muller, F., Pita, J.C., Howell, D.S., manicourt, D.H., 1986. Tensile properties of knee joint cartilage. I. influence of ionic conditions, weight bearing and fibrillation on the tensile modulus. Journal of Orthopaedic Reseach 4, 379-392.

[17] Bonifasilista, C. , Lake, S. P. , Small, M. S. , & Weiss, J. A. . (2010). Viscoelastic properties of the human medial collateral ligament under longitudinal, transverse and shear loading. *Journal of Orthopaedic Research, 23*(1), 67-76.

[18] https://teachmeanatomy.info/upper-limb/joints/shoulder/

[19] Bigliani, L. U. , Pollock, R. G. , Soslowsky, L. J. , Flatow, E. L. , Pawluk, R. J. , & Mow, V. C. . (1992). Tensile properties of the inferior glenohumeral ligament. *Journal of Orthopaedic Research, 10*(2), 187-197.

[20] Ticker, J. B. , Bigliani, L. U. , Soslowsky, L. J. , Pawluk, R. J. , Flatow, E. L. , & Mow, V. C. . (1996). Inferior glenohumeral ligament: geometric and strain-rate dependent properties *. J Shoulder Elbow Surg, 5(4), 269-279.

[21] Lee, T. Q. , Dettling, J. , Sandusky, M. D. , & Mcmahon, P. J. . (1999). Age related biomechanical properties of the glenoid-anterior band of the inferior glenohumeral ligament-humerus complex. *Clinical Biomechanics, 14*(7), 471-476.

[22] Pollock, R. G. , Wang, V. M. , Bucchieri, J. S. , Cohen, N. P. , Huang, C. Y. , & Pawluk, R. J. , et al. (2000). Effects of repetitive subfailure strains on the mechanical behavior of the inferior glenohumeral ligament. Journal of Shoulder & Elbow Surgery, 9(5), 427-435.

[23] McKeen, & Laurence, W. . (2014). The effect of long term thermal exposure on plastics and elastomers || introduction to the physical, mechanical, and thermal properties of plastics and elastomers. 43-71.

[24] Mckeen, L. W. . (2014). 1 – introduction to plastics, polymers, and their properties. Effect of Temperature & Other Factors on Plastics & Elastomers, 1-45.

[25] http://www.tainstruments.com.cn/q800/ The brochure of DMA Q800

[26] Spiegelberg, S. . (2009). Characterization of physical, chemical, and mechanical properties of uhmwpe-chapter 12. *Uhmwpe Handbook*, 355-368.

[27] Standard Test Method for Tensile Properties of Plastics. *ASTM international, ASTM D638-14*. ASTM international, 100 Barr Harbour Dr. P.O. box C-700 West Conshohocken, Pennsylvania United States.

[28] Standard Test Methods and Definitions for Mechanical Testing of Steel Products. *ASTM international, A370-17a*. ASTM international, 100 Barr Harbour Dr. P.O. box C-700 West Conshohocken, Pennsylvania United States.

[29] Standard Test Methods for Tension Testing of Metallic Materials. *ASTM international, ASTM E8/E8M-16a*. ASTM international, 100 Barr Harbour Dr. P.O. box C-700 West Conshohocken, Pennsylvania United States.

[30] *ISO 572*. Textile machinery and accessories -- Shuttles for pirn changing automatic looms – Dimensions. 1976